Measuring flavor ratios of high-energy astrophysical neutrinos

John F. Beacom,[1,*] Nicole F. Bell,[1,2,†] Dan Hooper,[3,‡] Sandip Pakvasa,[4,2,§] and Thomas J. Weiler[5,2,‖]
[1]*NASA/Fermilab Astrophysics Center, Fermi National Accelerator Laboratory, Batavia, Illinois 60510-0500, USA*
[2]*Kavli Institute for Theoretical Physics, University of California, Santa Barbara, California 93106, USA*
[3]*Department of Physics, University of Wisconsin, Madison, Wisconsin 53706, USA*
[4]*Department of Physics and Astronomy, University of Hawaii, Honolulu, Hawaii 96822, USA*
[5]*Department of Physics and Astronomy, Vanderbilt University, Nashville, Tennessee 37235, USA*
(Received 1 July 2003; published 11 November 2003)

We discuss the prospects for next generation neutrino telescopes, such as IceCube, to measure the flavor ratios of high-energy astrophysical neutrinos. The expected flavor ratios at the sources are $\phi_{\nu_e}:\phi_{\nu_\mu}:\phi_{\nu_\tau}=1:2:0$, and neutrino oscillations quickly transform these to 1:1:1. The flavor ratios can be deduced from the relative rates of showers (ν_e charged current, most ν_τ charged current, and all flavors neutral current), muon tracks (ν_μ charged current only), and tau lepton lollipops and double bangs (ν_τ charged current only). The peak sensitivities for these interactions are at different neutrino energies, but the flavor ratios can be reliably connected by a reasonable measurement of the spectrum shape. Measurement of the astrophysical neutrino flavor ratios tests the assumed production mechanism and also provides a very long baseline test of a number of exotic scenarios, including neutrino decay, *CPT* violation, and small-δm^2 oscillations to sterile neutrinos.

DOI: 10.1103/PhysRevD.68.093005 PACS number(s): 95.85.Ry, 13.35.Hb, 14.60.Pq, 96.40.Tv

I. INTRODUCTION

A new generation of detectors proposed or already under construction will have the sensitivity to open a new window on the Universe in the form of high-energy neutrino astronomy. In addition to probing distant and mysterious astrophysical sources, these data will offer unprecedented sensitivity for testing fundamental neutrino properties.

Under-ice and underwater optical Cerenkov detectors are sensitive at roughly TeV–PeV neutrino energies. The Antarctic Muon and Neutrino Detector Array (AMANDA) [1] at the South Pole has already been taking data for several years, as has the smaller Lake Baikal detector [2]. First results from the AMANDA-B10 phase have been reported [1,3], and results from several years of running in the larger AMANDA-II configuration [4] are eagerly awaited. Construction of the much larger (km^3) IceCube detector [5] at the South Pole is scheduled to begin later this year. The ANTARES [6] and NESTOR [7] Collaborations, drawing on the lessons learned by the Deep Underground Muon and Neutrino Dectector (DUMAND) project [8], are currently deploying their detectors in the Mediterranean Sea. While smaller than IceCube, these detectors will have lower thresholds due to denser instrumentation. Another Mediterranean detector, NEMO [9], has been proposed. These detectors operate underwater or under ice to shield the atmospheric muon flux; since they primarily look for upgoing neutrino-induced events, the detectors in the southern and northern hemispheres offer complementary views of the sky.

Detectors making use of the Earth's atmosphere as a target volume are sensitive at roughly EeV–ZeV neutrino energies. Fly's Eye [10] and the Akeno Giant Air Shower Array (AGASA) [11], designed to detect atmospheric showers induced by cosmic ray protons, are also sensitive to ultra-high-energy neutrino primaries if they consider penetrating horizontal showers, i.e. events that initiate only at great slant depth in the atmosphere. The bounds on ultra-high-energy neutrino fluxes are reviewed in Ref. [12]. The HiRes detector (an upgrade of Fly's Eye) is running [13] and the Pierre Auger detector [14], scheduled to be completed in 2005, is already taking data with its engineering array. Both should significantly improve the sensitivity to ultra-high-energy astrophysical neutrinos. Orbiting detectors will soon provide a new window on neutrinos as well. The EUSO experiment [15] is scheduled for deployment on the International Space Station in early 2009, and it may evolve into a larger satellite mission named OWL [16].

Radio Cerenkov detectors are sensitive at roughly PeV–ZeV neutrino energies. As pointed out long ago by Askaryan [17], a Cerenkov signal is proportional to the square of the net charge of the shower within a wavelength. In turn, the net charge is roughly proportional to the shower energy. Thus, the long-wavelength radio signal rises as the neutrino energy squared, instead of just the neutrino energy, as for other techniques. The RICE antennas, co-deployed with AMANDA, have recorded first results [18]. Recently, NASA approved a very interesting experiment, ANITA [19], which will carry radio antennas on a balloon above the South Pole in an attempt to detect the long-wavelength tail of sub-ice showers from Earth-skimming neutrinos [20]. The GLUE experiment has reported limits based on the non-observation of a radio signal from neutrino interactions in the surface of the Moon [21]. The proposed SALSA detector [22] could use large salt domes as a radio Cerenkov medium.

Although the goals of these experiments are common, the detection strategies and systematic issues are not. Each will infer the direction of arriving events, thereby enabling point-

*Electronic address: beacom@fnal.gov
†Electronic address: nfb@fnal.gov
‡Electronic address: hooper@pheno.physics.wisc.edu
§Electronic address: pakvasa@phys.hawaii.edu
‖Electronic address: tom.weiler@vanderbilt.edu

 ©2003 The American Physical Society

source neutrino astronomy. Each will measure the neutrino flux over some energy range. One purpose of this paper is to ask how well the primary neutrino spectrum can be reconstructed from the observed spectral information. The primary spectrum reveals the dynamics of the cosmic engine. Reviews of high-energy neutrino astronomy are listed in Ref. [23].

Besides energy and direction, an additional piece of information is carried by arriving neutrinos: flavor. Neutrinos are known to come in three flavors, electron, muon, and tau types. The bulk of this paper focuses on what we can learn from flavor identification of the incoming neutrinos and whether flavor-tagging is feasible with proposed experiments. We consider the IceCube experiment in detail due to its large effective volume and ability to observe showers, muon tracks and events unique to tau neutrinos. We emphasize that other experiments will also have some capabilities to discriminate among neutrino flavors.

In the next section, we look at theoretical motivations for flavor discrimination. In the sections after, we look at the inferences of the incident neutrino spectrum and the neutrino flavors from various event signatures.

II. WHY NEUTRINO FLAVOR IDENTIFICATION IS INTERESTING

Neutrinos from astrophysical sources are expected to arise dominantly from the decays of charged pions (and kaons) and their muon daughters, which results in initial flavor ratios, $\phi_{\nu_e}:\phi_{\nu_\mu}:\phi_{\nu_\tau}$, of nearly 1:2:0. The fluxes of each mass eigenstate are then given by $\phi_j=\Sigma_\alpha \phi_{\nu_\alpha}^{\rm source}|U_{\alpha j}|^2$. The $U_{\alpha j}$ are elements of the neutrino mass-to-flavor mixing matrix, defined by $|\nu_\alpha\rangle=\Sigma_j U_{\alpha j}|\nu_j\rangle$. The propagating mass eigenstates acquire relative phases, giving rise to flavor oscillations. However, these relative phases are lost, since $\delta m^2 \times L/E \gg 1$, and hence uncertainties in the distance L and the energy E will wash out the relative phases. Thus the neutrinos arriving at Earth are an incoherent mixture of mass eigenstates with the proportions given above.

For three neutrino species, as we assume throughout, there is now strong evidence from atmospheric and reactor neutrino data suggesting that ν_μ and ν_τ are maximally mixed and U_{e3} is nearly zero. This twin happenstance ($\theta_{\rm atm}=45°$ and $U_{e3}=0$) leads to two remarkable conclusions. The first is that each mass eigenstates contains an equal fraction of ν_μ and ν_τ. The second is that in the mass eigenstate basis, the neutrinos are produced in the ratios 1:1:1, independent of the solar mixing angle, and thus arrive at Earth as an incoherent mixture of mass eigenstates with these same ratios. This implies democracy in the detected flavor ratios as well, since $U\mathbb{1}U^\dagger=\mathbb{1}$ in any basis.

So there is a fairly robust prediction of 1:1:1 flavor ratios for measurements of astrophysical neutrinos [24,25]. The first task of flavor measurement is to check this prediction. Could the flavor ratios differ from 1:1:1? The astrophysics could be different than is outlined here. For example, if the charged pion decays promptly but the daughter muon loses energy before decaying, then at high energy the flux may approximate $\phi_{\nu_e}:\phi_{\nu_\mu}:\phi_{\nu_\tau}\sim 0:1:0$ [26]. This leads to mass eigenstate ratios of $\sim 1:2:3$ and measured flavor ratios of $\sim 1:2:2$.

Alternatively, the particle physics could be different than assumed here (three stable neutrinos). For example, the heavier mass eigenstates could decay en route to Earth. This leads to markedly different detected flavor ratios, as extreme as either 6:1:1 or 0:1:1 for the normal and inverted hierarchies, respectively [27]. Also, Barenboim and Quigg have pointed out that *CPT* violation in neutrino mixing could also lead to anomalous flavor ratios [28]. Finally, neutrinos could be pseudo-Dirac states, in which case the three active neutrinos have sterile partners, with which they are maximally mixed with very tiny δm^2 splittings; these oscillations might only be effective over cosmological distances [29].

In all cases investigated, the ν_μ-ν_τ symmetry ensures that ν_μ and ν_τ arrive at Earth in equal numbers. Given how robust that prediction is and that ν_τ is the most difficult flavor to identify in IceCube, we will mostly focus on the $\phi_{\nu_e}:\phi_{\nu_\mu}$ ratio. We will show that this can be determined by measuring the rates of shower and track events in IceCube. Additionally, we discuss the identification of ν_τ; though the expected yields are very small, the signals are very distinctive, and the detection of even a single event would confirm the presence of the ν_τ flux.

III. BASICS FIRST: MEASURING THE NEUTRINO SPECTRUM WITH MUONS

For under-ice or underwater detectors, muon events provide the most useful signal from which to infer the neutrino spectrum. This is especially true at lower energies (from 100 GeV to several TeV) due to the higher energy threshold for showers. In this section we explore the reconstruction of the neutrino spectrum from observed muon events in an IceCube-type detector. There are challenges in doing this, however.

First, muons can be created in interactions far from the detector and lose a considerable fraction of their energy before being measured. This problem can be circumvented, however, by considering only muon events with a contained vertex, in which the muon track begins within the detector volume. At energies near or below the TeV scale, many of the observed muons will have contained vertices. At higher energies, when the range of muons is considerably longer, fewer of the resulting events will have this feature.

Second, separating the atmospheric neutrino background from any astrophysical neutrino signal can be difficult. The atmospheric neutrino spectrum is well modeled, and so in principle can be subtracted from the data. At energies at or above about 100 TeV, the astrophysical neutrino flux is likely to be above the more steeply falling atmospheric neutrino flux. At more modest energies, the angular and temporal resolution of a neutrino telescope will be needed to effectively remove backgrounds. The atmospheric neutrino flux at 1 TeV (dominated by $\nu_\mu+\overline{\nu}_\mu$) is $\sim 10^{-8}$ GeV cm^{-2} s^{-1} [30] in a (1 deg)^2 bin, where the bin size was chosen to reflect the angular resolution for these events. Especially for

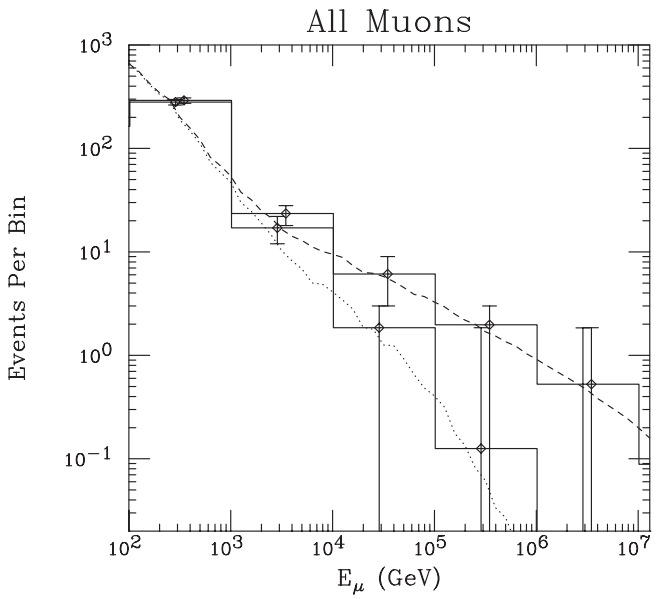

FIG. 1. The distribution of observed muon energies for a neutrino spectrum of $E^2_{\nu_\mu} dN_{\nu_\mu}/dE_{\nu_\mu} = 10^{-7}$ GeV cm^{-2} s^{-1} for 1 year. The dashed line is for a flux at a horizontal zenith angle and the dotted line for an upgoing flux (through the Earth). Note that the muon energy at production may be considerably larger than that observed due to the long muon range. The error bars are slightly offset for clarity.

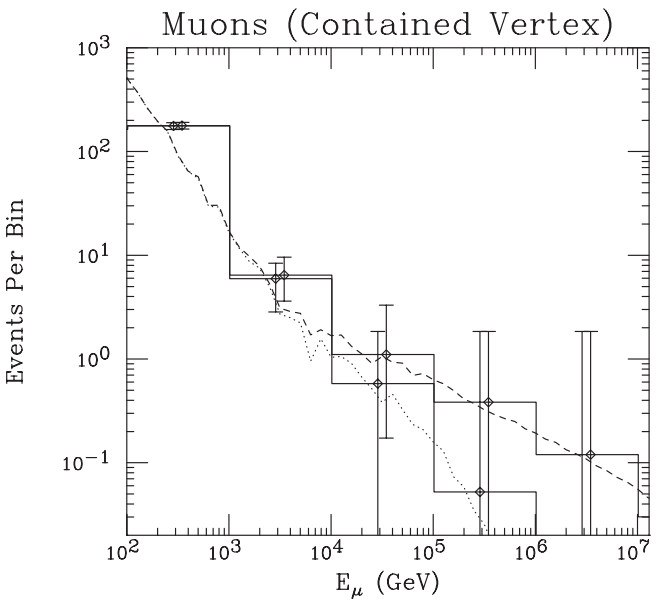

FIG. 2. The distribution of observed *contained vertex* muon energies for a neutrino spectrum of $E^2_{\nu_\mu} dN_{\nu_\mu}/dE_{\nu_\mu} = 10^{-7}$ GeV cm^{-2} s^{-1} for 1 year. The dashed line is for a flux at a horizontal zenith angle and the dotted line for an upgoing flux (through the Earth). The error bars are slightly offset for clarity.

the lower flux we consider below, identification of astrophysical sources may require temporal information as well. For example, gamma-ray bursts typically have durations on the order of seconds. Taking the known catalogs of gamma-ray bursts as a guide, about 10 events per square kilometer per year are expected. Using timing and directional information, these events are essentially background free [31]. Tau neutrino detection for gamma-ray bursts has been studied in Ref. [32]. A similar technique could be used for blazars or other transient sources.

A. Muon tracks

After a high energy muon is produced, it undergoes continuous energy loss as it propagates, given by

$$\frac{dE}{dX} = -\alpha - \beta E, \tag{3.1}$$

where $\alpha = 2.0$ MeV cm^2/g and $\beta = 4.2 \times 10^{-6}$ cm^2/g [33]. The muon range is then

$$R_\mu = \frac{1}{\beta} \ln\left[\frac{\alpha + \beta E_\mu}{\alpha + \beta E_\mu^{\rm thr}}\right], \tag{3.2}$$

where $E_\mu^{\rm thr}$ is the minimum muon energy triggering the detector. Typically, $E_\mu^{\rm thr} \sim 50$–100 GeV for deep ice or water detectors. Above an energy of 1 TeV, the muon range rises logarithmically as $\sim \ln(E_\mu/E_\mu^{\rm thr})$ times 2.4 km water equivalent. Since this typically exceeds the size of the detector, the muon energy cannot be measured by the muon range. Further, since the muons are always fully relativistic, the Čerenkov angle and intensity are constant and thus cannot be used to infer the muon energy. However, the muon energy inside the detector can be inferred by the rate of energy deposition in the form of showers from catastrophic bremsstrahlung [5,34]. The muon range is substantially less than the muon decay length; for an illustration of the length scales for neutrino interactions, mu and tau range, and mu and tau decay, see Fig. 1 of Ref. [35].

The energy of the muon faithfully represents the neutrino energy since the charged-current differential cross section is strongly peaked at $y = 1 - E_\mu/E_\nu \simeq 0$, and $\langle y \rangle \simeq 0.2$ [36]. The kinematical angle of the muon relative to the neutrino direction is about $1^\circ/\sqrt{E_\nu/1\ \text{TeV}}$, and the reconstruction error on the muon direction is on the order of 1°.

The probability of detecting a muon neutrino traveling through the detector via a charged-current interaction is then given by

$$P_{\nu_\mu \to \mu} \simeq \rho N_A \sigma R_\mu, \tag{3.3}$$

where ρ is the target nucleon density, N_A is Avogadro's number, and σ is the neutrino-nucleon total cross section [36].

B. Spectral results

In Figs. 1 and 2, we show the distribution of observed muon energies for a muon neutrino spectrum of $E^2_{\nu_\mu} dN_{\nu_\mu}/dE_{\nu_\mu} = 10^{-7}$ GeV cm^{-2} s^{-1} for 1 year (or $E^2_{\nu_\mu} dN_{\nu_\mu}/dE_{\nu_\mu} = 10^{-8}$ GeV cm^{-2} s^{-1} for 10 years). The dashed lines correspond to the flux at a horizontal zenith angle and the dotted lines to an upgoing flux (through the Earth). Detection prospects for horizontal neutrinos are en-

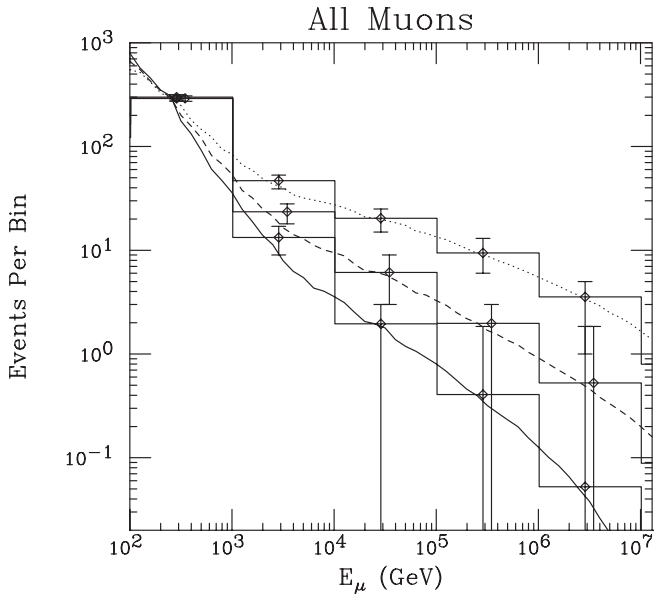

FIG. 3. The distribution of observed muon energies for a neutrino spectrum of $E^2_{\nu_\mu} dN_{\nu_\mu}/dE_{\nu_\mu} = 10^{-7}$ GeV cm^{-2} s^{-1} for 1 year (dashed line), as in Figs. 1 and 2, compared against spectra proportional to $E^{-2.2}$ (solid line) and $E^{-1.8}$ (dotted line), normalized to the same number of events in the first energy bin. All rates are for a horizontal zenith angle source. Note that the muon energy at production may be considerably larger than that observed. The error bars are slightly offset for clarity.

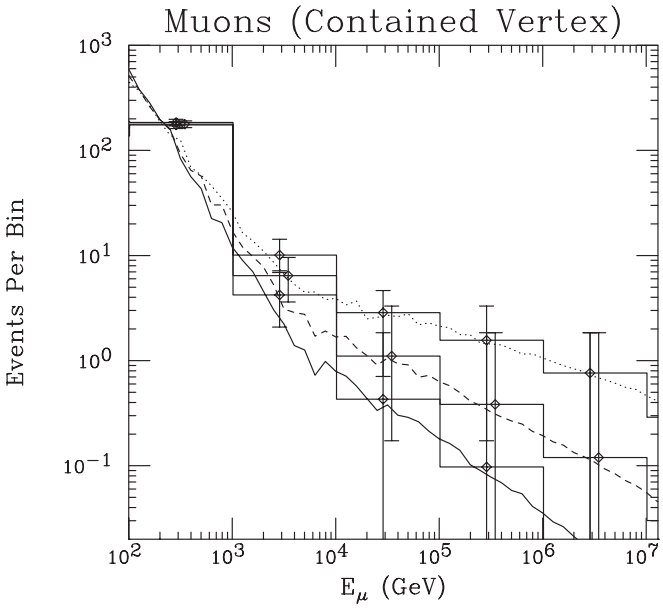

FIG. 4. The distribution of observed *contained vertex* muon energies for a neutrino spectrum of $E^2_{\nu_\mu} dN_{\nu_\mu}/dE_{\nu_\mu} = 10^{-7}$ GeV cm^{-2} s^{-1} for 1 year (dashed line), as in Figs. 1 and 2, compared against spectra proportional to $E^{-2.2}$ (solid line) and $E^{-1.8}$ (dotted line), normalized to the same number of events in the first energy bin. All rates are for a horizontal zenith angle source. The error bars are slightly offset for clarity.

hanced from long distances of ice in which muons can be produced. Upgoing neutrinos, although also with this advantage, can be absorbed in the Earth, degrading their event rate. A distribution of neutrino sources over the sky produces a spectrum in between these two extreme curves. Figure 1 shows the spectrum of all observed muons, while Fig. 2 shows only muon events with a contained vertex. The events are binned by energy decade, with 68% confidence levels shown. The dashed and dotted lines, shown for comparison, are the results of our Monte Carlo simulations with much greater statistics. Note that the sizes of the energy bins were selected for statistical purposes. The energy resolution of neutrino telescopes is considerably more precise at these energies.

In Figs. 3 and 4, we compare the observable horizontal muon spectra resulting from neutrino spectra proportional to E^{-2} (dashed line), $E^{-2.2}$ (solid line), and $E^{-1.8}$ (dotted line), normalized to the same number of events in the first energy bin. By comparing the numbers of events in adjacent bins, Fig. 3 demonstrates that for a single power-law flux (and our choice of normalization), the spectral slope can be determined to approximately 10% up to tens or perhaps hundreds of TeV. Figure 4 demonstrates the ability to make such measurements with only muons with contained vertices. Comparing Figs. 3 and 4 makes it clear that limiting the data to muons with contained vertices alone weakens the ability to resolve similar spectral slopes, especially at higher energies. This is because of the statistical limitations. However, the fact that muons with contained vertices yield the total muon energy, whereas throughgoing muons offer only lower limits to the energy, has its virtue. The contained-muon measurement is more useful for the case of a strongly broken power law, such as is predicted in the case of gamma-ray bursts. Typically, the gamma-ray burst neutrino spectrum is expected to follow a E^{-1} spectrum up to some break energy on the order of hundreds of TeV. Above this energy, it steepens to a spectrum proportional to E^{-2}. For such a spectrum, the break could be observed with the contained vertex muon measurement, and the slopes could be then measured more precisely using all observed muons.

We note that the flux we employ for illustration, $E^2_{\nu_\mu} dN_{\nu_\mu}/dE_{\nu_\mu} = 10^{-7}$ GeV cm^{-2} s^{-1}, is on the order of the Waxman-Bahcall bound [37]. The Waxman-Bahcall bound pertains to the diffuse neutrino flux from sources optically thin to protons, normalized to the measured cosmic-ray flux at $\sim 10^{18}$ eV. As emphasized by Mannheim, Protheroe and Rachen [38], it does not apply for optically thick or ''hidden'' sources [39], for galactic sources, or for sources not emitting protons at energies $\sim 10^{18}$ eV. Microquasars and supernova remnants provide examples of both of the latter categories. The current experimental limit on the high-energy neutrino flux, from the AMANDA experiment, is more than an order of magnitude larger than the Waxman-Bahcall bound [1,3]. IceCube is expected to reach well below the Waxman-Bahcall bound [5].

Nature's flux could be larger than we assume here. It could also be smaller. If it is smaller, then integration times larger than the 1 year we assume here are needed to compensate. Furthermore, larger detectors, such as an extension of IceCube, are likely to be constructed in the future, making

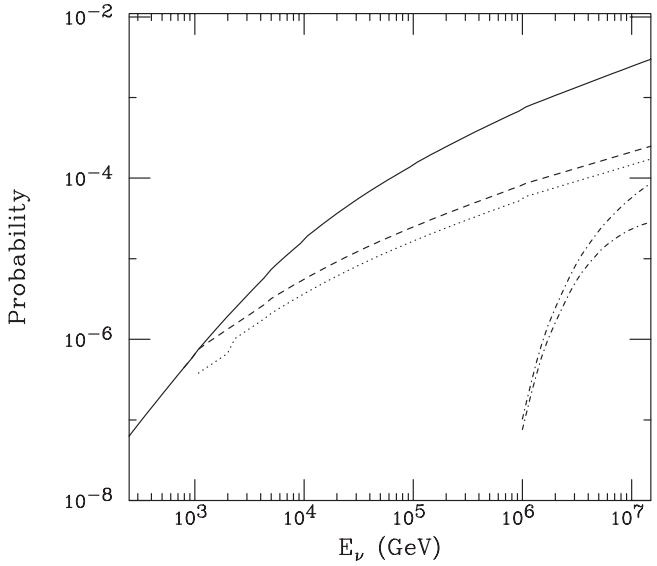

FIG. 5. Probabilities of detecting different flavors of neutrinos in IceCube versus neutrino energy, described in detail in the text. The upper solid line is the probability of a horizontal ν_μ creating a detectable muon track, and the dashed line is for downgoing ν_μ. The dotted line is the probability for ν_e to create a detectable shower (above 1 TeV), considering both charged-current and neutral-current interactions; the kink occurs when the neutral-current showers come above threshold. The dot-dashed lines are the probabilities for ν_τ to make lollipop events (upper) and double-bang events (lower).

more conservative choices of the neutrino flux easier to study. To reduce backgrounds, only those events associated with known sources should be considered. In that case, the remaining flux of neutrinos which could be used for such a study may be significantly reduced. Given this consideration, perhaps a choice of $E^2_{\nu_\mu} dN_{\nu_\mu}/dE_{\nu_\mu} = 10^{-8}$ GeV cm^{-2} s^{-1} over 10 years, which we also discuss, could be considered a more realistic choice.

IV. FLAVOR IDENTIFICATION

Although the ratios of neutrino flavors are not directly measurable, they can be inferred from complementary classes of events in neutrino telescopes. In this section, we restrict our attention to IceCube, which will be capable of identifying showers from both charged- and neutral-current events, muon tracks, and certain tau neutrino events. Muon tracks have been discussed above. The probabilities for detecting the different neutrino flavors are illustrated in Fig. 5, and will be discussed in detail now.

Electron and muon neutrinos above about 100 TeV are absorbed in Earth by their charged-current interactions. Tau neutrinos also interact, but regenerate ν_τ by the prompt decays of tau leptons [40]; these decays also produce a secondary flux of ν_e and ν_μ [35,41].

A. Showers

All neutrino flavors undergo an identical neutral-current interaction producing a hadronic shower and nothing else. The shower energy typically underestimates the neutrino energy by a factor ranging from ~ 3 around 1 TeV to a factor of ~ 4 at 1 EeV [36].

A charged-current interaction of ν_e produces an electron that immediately creates an electromagnetic shower. If the electromagnetic shower is measured with the hadronic one, the total shower energy is the incident ν_e energy. In principle, electromagnetic and hadronic showers are distinguishable by their respective muon content, absent for electromagnetic and present for hadronic showers. We will not assume that these can be distinguished, as it is expected to be very difficult.

In a ν_μ charged-current interaction, the muon track always emerges from the shower, because of the long muon range, so these events do not contribute to the shower rate.

The ν_τ charged-current interaction produces a hadronic shower and a tau track. The tau decay path length is $\gamma c\tau \sim 50(E_\tau/\text{ PeV})$ m. Below a few PeV, the tau track is too short to be separated from the shower, and so these events will contribute to the shower rate. At higher energies, the tau track will extend beyond the initial shower, and then the tau will decay to produce a second shower. This creates identifiable double-bang and lollipop events, discussed below.

Showers are seen by the detector as photoelectrons distributed over a ~ 100 m radius sphere for a TeV shower (~ 300 m radius for showers with PeV energies). The shower must at least be partially contained within the detector volume in order to be detected. Since shower sizes are relatively small compared to muon ranges, the effective volume for these events is substantially less than for charged-current ν_μ interactions. Also, the energy threshold for showers is generally larger than for muon tracks.

The probability of detecting a neutrino by a shower produced by a neutral-current interaction is given by

$$P_{\nu\to\text{shower}} \simeq \rho N_A L \int_{E^{\text{thr}}_{\text{sh}}/E_\nu}^{1} \frac{d\sigma}{dy} dy \tag{4.1}$$

where σ is the neutrino-nucleon cross section [36], y is the energy fraction transferred from the initial neutrino to the hadronic shower, and L is the length of the detector. For charged-current electron neutrino interactions, however, the additional electromagnetic shower means that all of the neutrino energy goes into the shower, and

$$P_{\nu\to\text{shower}} \simeq \rho N_A \sigma L. \tag{4.2}$$

A similar treatment is used for charged-current tau neutrino interactions which do not produce a double-bang or lollipop event (see below). In real experiments, the shower threshold is not a step function as we adopt here. IceCube will have shower energy resolution of about ± 0.1 on a $\log_{10}$ scale and will be able to reconstruct the neutrino direction to about 25°.

B. Double-bang and lollipop events

Double-bang and lollipop events are signatures unique to tau neutrinos, made possible by the fact that tau leptons decay before they lose a significant fraction of their energy

[33]. Double-bang events [24,42,43] consist of a hadronic shower initiated by a charged-current interaction of the ν_τ followed by a second energetic shower (hadronic or electromagnetic) from the decay of the resulting tau lepton. Lollipop events consist of the second of the two double-bang showers along with the reconstructed tau lepton track (the first bang may be detected or not). Inverted lollipops, consisting of the first of the two double-bang showers along with the tau lepton track, are not as useful as they will often be confused with a hadronic shower in which a $\sim$100 GeV muon is produced (because of the higher lepton mass, tau tracks suffer much less catastrophic bremsstrahlung than muons at the same energy). We do not consider inverted lollipops for this reason.

The range of a tau lepton is bounded from above by its lifetime in the laboratory frame. A tau lepton of energy E_τ has a mean lifetime given by

$$R_\tau(E_{\nu_\tau},y)=\frac{E_\tau}{m_\tau}c\tau_\tau=\frac{(1-y)E_{\nu_\tau}}{m_\tau}c\tau_\tau, \tag{4.3}$$

where m_τ and τ_τ are the mass and rest-frame lifetime.

Following Refs. [24,42,43], the conditions which must be fulfilled for the detection of a double-bang event are the following:

(i) The tau neutrino must interact via the charged current, producing a hadronic shower of sufficient energy to trigger the detector ($\sim$1 TeV) inside of the detector volume.
(ii) The tau lepton produced in the interaction must decay inside the detector volume, producing an electromagnetic or hadronic shower of sufficient energy to trigger the detector.
(iii) The tau lepton must travel far enough such that the two showers are sufficiently separated to be distinguished from each other

At the energies required for the third condition to be satisfied, both the showers will be energetic enough to easily fulfill the threshold requirements. The probability for a double-bang event, per incident tau neutrino, is

$$P_{\rm db}(E_{\nu_\tau})\simeq\rho N_A\int_0^1 dy\frac{d\sigma}{dy}\int_{x_{\rm min}}^L dx\,\frac{(L-x)}{R_\tau}e^{-x/R_\tau}$$

$$\simeq\rho N_A\int_0^1 dy\frac{d\sigma}{dy}[(L-x_{\rm min}-R_\tau)e^{-x_{\rm min}/R_\tau}+R_\tau e^{-L/R_\tau}]. \tag{4.4}$$

The track integration from $x_{\rm min}$ to L includes tau lengths that are larger than $x_{\rm min}$ (for shower separation) and smaller than L (so that both showers are contained in the detector). The exponential in the integral samples over the decay length distribution.

Conditions which must be fulfilled for the detection of a lollipop event are the following:

(i) The shower produced by the decay of the tau lepton must occur within the detector volume and be of sufficient energy to trigger the detector ($\sim$1 TeV). This may be a hadronic or electromagnetic shower.
(ii) The track of the tau lepton must be long enough (within the detector) to be reconstructed and separable from the shower. For a photomultiplier tube spacing of $\sim$125 m (IceCube's horizontal spacing is 125 m, their vertical spacing is a significantly smaller 17 m), reasonable values for the minimum tau range, $x_{\rm min}$, are 200–400 m.

The probability for a lollipop event, per incident tau neutrino, is

$$P_{\rm lollipop}(E_{\nu_\tau})\simeq\rho N_A(L-x_{\rm min})\int_0^1 dy\frac{d\sigma}{dy}e^{-x_{\rm min}/R_\tau}. \tag{4.5}$$

Note that the energy threshold for both double bangs and lollipops, resulting from the requirement $R_\tau\gtrsim x_{\rm min}$, is given by $E_{\nu_\tau}^{\rm thr}\sim 5(x_{\rm min}/250\ {\rm m})$ PeV. For double-bang events, the energy threshold for the first shower, $E_{\rm sh}\sim yE_{\nu_\tau}\gtrsim$TeV, puts a lower limit on the y integration, but negligibly so for PeV scale neutrino energies.

The expressions in Eqs. (4.4) and (4.5) can be further simplified with the approximation

$$\frac{d\sigma}{dy}\simeq\sigma\delta(y-\langle y\rangle), \tag{4.6}$$

where $\langle y\rangle\simeq 0.25$ at PeV scale energies and σ is the total cross section. Thus,

$$P_{\rm db}(E_{\nu_\tau})\simeq\rho N_A\sigma[(L-x_{\rm min}-R_\tau)e^{-x_{\rm min}/R_\tau}+R_\tau e^{-L/R_\tau}]_{y=\langle y\rangle}, \tag{4.7}$$

$$P_{\rm lollipop}(E_{\nu_\tau})\simeq\rho N_A\sigma(L-x_{\rm min})[e^{-x_{\rm min}/R_\tau}]_{y=\langle y\rangle}. \tag{4.8}$$

Figure 6 shows the lollipop and double-bang detection probabilities. Note that near threshold, the majority of lollipop events are also double-bang events. At higher energies, the size of the detector excludes many double-bang events but not lollipops.

The analytic expressions in Eqs. (4.4)–(4.8) are original to this work. To check their validity, we constructed a Monte Carlo simulation to calculate the probabilities of observing double-bang or lollipop events in IceCube. This simulation took into account the distribution of y values in charged-current interactions as well as the variation in decay lengths. In common with the analytic results, the Monte Carlo simulation treats the detector one dimensionally. We note that this is a conservative approximation as taus that travel diagonally across the detector could have bangs separated by distances larger up to a factor $\sqrt{3}$. The analytic expressions and the

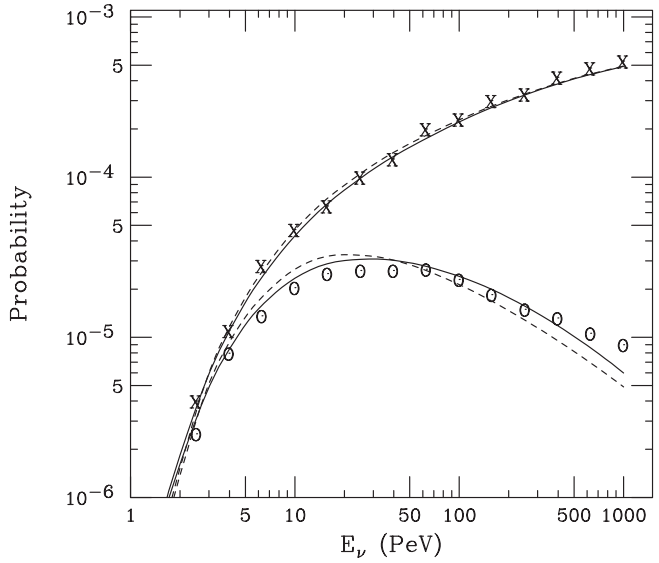

FIG. 6. Probability of observing a lollipop (upper) or double-bang (lower) event in IceCube per incident tau neutrino. The points (X's and O's) represent Monte Carlo results while the solid lines represents the analytic expressions of Eqs. (4.4) and (4.5) and the dashed lines represents the approximations of Eqs. (4.7) and (4.8). We have set $L=1$ km and $x_{\min}=250$ m. Above about 20 PeV, the tau track length becomes long enough that it may exceed the thickness of the ice for near-downgoing events, introducing zenith-angle dependence.

Monte Carlo calculation shown in Fig. 6 are in good agreement, a considerable improvement over the approximations given in Refs. [42,43]. In particular, the important threshold region is characterized very well. The remaining minor discrepancies we attribute to the low statistics of the Monte Carlo calculation; our formulas should be quite accurate. In addition, the approximation in Eq. (4.6) is seen to yield quite accurate results (which indicates that the variation of cross section with y is relatively unimportant in these calculations). Thus we have good confidence that Eqs. (4.4)–(4.8) may join with Eqs. (3.3)–(4.2) to complete the set of probabilities of event topologies.

C. Determining the muon/shower ratio

The spectrum of shower events is more difficult to infer from data than is the muon spectrum due to lower statistics, but it may be possible [44]. Relative disadvantages are the considerably higher shower energy threshold [5] and the fact that muon event rates benefit from long muon ranges. However, in contrast to the muon signals, shower events are produced by all flavors of neutrinos, and shower energies more faithfully represent the neutrino energy than do muon tracks. We do not attempt to relate the observed shower spectrum to the spectrum of incident neutrinos. Rather, we assume that, due to oscillations, the neutrino spectrum shape is independent of flavor; i.e., the neutrino spectrum inferred from a measurement of the muon spectral shape is universal. We may use this universal spectrum to produce shower events and muon tracks, and then compare the total number of shower events to the total number of muon events to obtain the flavor ratios. Recall that ν_μ-ν_τ symmetry means $\phi_{\nu_\mu}:\phi_{\nu_\tau}=1:1$, and so two independent observables are sufficient to determine all three flavor ratios.

For a neutrino spectrum of $E^2_{\nu_\mu} dN_{\nu_\mu}/dE_{\nu_\mu} = 10^{-7}$ GeV cm^{-2} s^{-1} for 1 year, we expect, on average, 323 muon events (186 of which have contained vertices). Given an equal number of each neutrino flavor, we predict only 36 shower events. At the 68% confidence level, this allows for a measurement of $N_{\text{muons}}/N_{\text{showers}}=9.0^{+1.6}_{-1.9}$ for horizontal sources, about a 20% uncertainty. For upgoing sources, a measurement of $N_{\text{muons}}/N_{\text{showers}}=8.5^{+1.5}_{-1.8}$ results similarly. The difference comes from the fact that upgoing neutrinos are absorbed at high energies, where muon events are more likely to occur, thus slightly lowering the muon to shower ratio for upgoing events relative to horizontal events. These results use the natural energy thresholds of the detector, $\sim$100 GeV for muons and $\sim$1 TeV for showers.

D. Signatures unique to tau neutrinos

Given the flux we have considered in this paper, $E^2_{\nu_\mu} dN_{\nu_\mu}/dE_{\nu_\mu}=10^{-7}$ GeV cm^{-2} s^{-1} for 1 year, we predict on the order of a 50% chance of observing a lollipop event and similarly for a double-bang event. Thus IceCube is unlikely to provide a stringent probe of the tau neutrino flux. The lack of observed double bangs or lollipops in IceCube would not reveal much, though the positive identification of even a single such event by IceCube would indicate the important existence of a tau neutrino flux on the order of the flux we consider here.

Even larger detectors are needed to exploit the double-bang and lollipop features. With several of these events, flavor ratios could be easily reconstructed and the ν_μ-ν_τ symmetry tested. Since even larger detectors are even farther into the future, we do not consider the double-bang and lollipop signatures further in this work.

V. INFERRING NEUTRINO FLAVOR RATIOS

Although the neutrino flavor ratios are not directly accessible at neutrino telescopes, the indirect flavor information collected from such experiments, i.e., the ratios of muon, shower and tau-unique events, can be very useful in inferring flavor information.

In the previous section, we showed that for a neutrino spectrum of $E^2_{\nu_\mu} dN_{\nu_\mu}/dE_{\nu_\mu}=10^{-7}$ GeV cm^{-2} s^{-1} for 1 year, IceCube could determine the ratio of the muon events to shower events with uncertainties on the order of 20%. Given ν_μ-ν_τ symmetry, this ratio can be used to deduce the ratio of electron neutrinos to either muon or tau neutrinos. Clearly, precision measurements of these quantities are unlikely to be determined in this fashion. Fortunately, in some interesting theoretical scenarios, the predictions for deviations from a 1:1:1 flavor ratio are so extreme as to not require greater precision. The neutrino decay model [27] provides a splendid example of possibly large flavor deviations.

In Fig. 7, we show the relationship between the muon-to-shower ratio and ν_e fraction, assuming ν_μ-ν_τ symmetry and

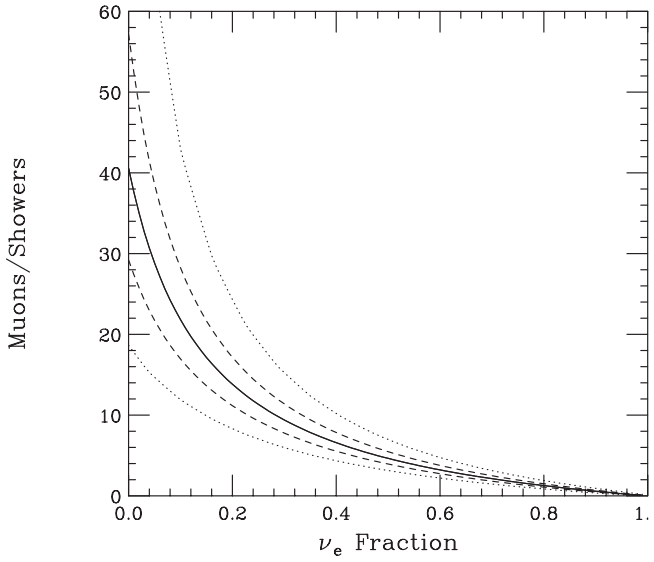

FIG. 7. The relationship between the muon-to-shower ratio and the ν_e fraction, assuming ν_μ-ν_τ symmetry and an E^{-2} power law spectrum. The muon energy threshold is 100 GeV, and the shower threshold is 1 TeV. Horizontal sources are assumed. The solid line is the central predicted value. The dashed lines represent the 68% confidence interval for a spectrum of $E^2_{\nu_\mu} dN_{\nu_\mu}/dE_{\nu_\mu} = 10^{-7}$ GeV cm^{-2} s^{-1} for 1 year. The dotted lines represent the 68% confidence interval for a spectrum 5 times smaller.

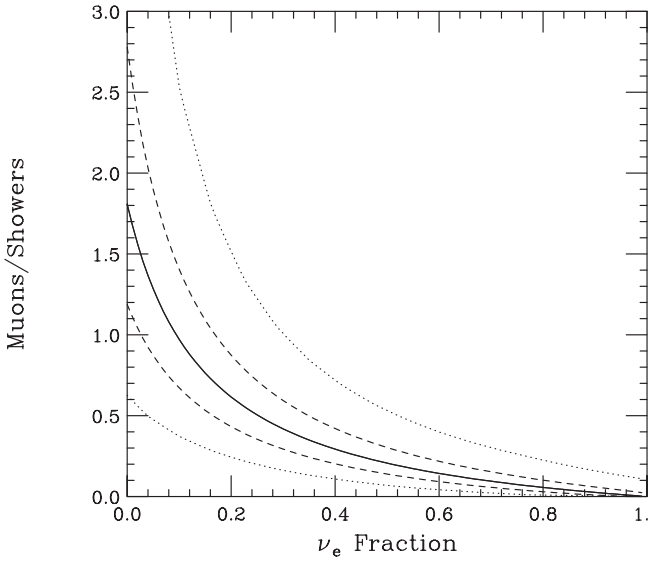

FIG. 8. Same as Fig. 7 except that a 1 TeV muon energy threshold has been imposed to reduce the effect of the uncertainty in the muon spectrum.

an E^{-2} power law spectrum. We define the ν_e fraction as the fraction of neutrinos with electron flavor (1 for all electron neutrinos, 0 for no electron neutrinos). The solid line is the central predicted value. The dashed lines represent the 68% confidence interval for our chosen spectrum. The dotted lines represent the 68% confidence interval for an exposure 5 times smaller. Note that the ν_e fraction of 1/3, expected from known particle physics, can be measured to a range of 0.26–0.37 or 0.18–0.44 for the two fluxes shown in Fig. 7, respectively. These measurements are sufficient to test interesting speculations such as neutrino decay.

If the neutrino spectrum is not well measured, then the relationship between the flavor ratios and the muon/shower ratio will be altered. In the case of poor muon spectrum resolution, some steps could be taken to reduce the related uncertainties. For example, the number of shower events could be compared to muon events above a threshold near 1 TeV, rather than the experimental threshold near 100 GeV. By doing this, the effect of the spectral slope is reduced, as shower events and muon events only from neutrinos with similar energies are compared. In Fig. 8, we show results analogous to Fig. 7, but with a muon energy threshold of 1 TeV imposed (Dutta, Reno, and Sarcevic [45] considered a shower/muon ratio to test three-flavor active neutrino oscillations against no oscillations, assuming standard flavor ratios at production; our results are in reasonable agreement at the one point of common consideration, a ν_e fraction of 1/3). With this choice of threshold, a measurement of $\alpha = 2.0 \pm 0.2$ corresponds to an uncertainty on the order of only 20% in the predicted muon/shower ratio. A ν_e fraction of 1/3 can be measured to a range of 0.22–0.42 or 0.09–0.61 for the two fluxes shown in Fig. 8, without using any information from muons below 1 TeV. With Fig. 7 as our guide, we summarize in Table I the muon-to-shower ratio expected for each of various astrophysical neutrino models.

VI. CONCLUSIONS

Next generation high energy neutrino telescopes, such as the kilometer scale experiment IceCube, will be capable of observing muon tracks produced by muon neutrinos, shower events from all flavors of neutrinos, and possibly the double-bang and lollipop topologies unique to tau neutrinos. Using these features, it will be possible to infer the flavor ratios of astrophysical neutrino fluxes. These can be used to probe properties of the sources [28] and to test for new physics beyond the standard model of neutrino physics [27–29].

Muon events, being the most numerous in under-ice and under-water detectors, are the most useful for measuring the astrophysical neutrino spectrum. We demonstrate that this can be accomplished with acceptable accuracy, given a sufficiently large but realistic neutrino flux. Knowledge of the spectral shape then allows us to make comparisons of the

TABLE I. Summary of the muon/shower ratios expected for selected scenarios. The decay scenarios with normal and inverted neutrino mass hierarchies are taken from Ref. [27].

Ratios at source	Decays	Ratios at Earth	ν_e fraction	Muon/shower (Fig. 7 central value)
1:2:0	None	1:1:1	0.33	9
	Normal	6:1:1	0.75	1.5
	Inverted	0:1:1	0	40
0:1:0	None	1:2:2	0.2	14

total number of event types (muons, showers, or tau-unique events) to infer the neutrino flavor ratios.

Assuming ν_μ-ν_τ symmetry as indicated by oscillation data, the ratio of showers to muons provides sufficient information to determine all three neutrino flavor ratios. Large deviations from the flavor ratios predicted by oscillations (1:1:1) will likely be observable. Furthermore, tau-unique events (double bangs and lollipops) provide another tool with which to address flavor identification; however, unless there is a larger than expected tau neutrino flux, such events will probably be too small in number in kilometer-scale detectors to provide useful information beyond the existence of astrophysical tau neutrinos.

ACKNOWLEDGMENTS

We thank Steve Barwick, Doug Cowen, Peter Gorham, Francis Halzen, and John Learned for valuable discussions. J.F.B. and N.F.B. were supported by Fermilab (operated by URA under DOE contract DE-AC02-76CH03000) and by NASA grant NAG5-10842. D.H. was supported by DOE grant DE-FG02-95ER40896 and the Wisconsin Alumni Research Foundation, S.P. by DOE grant DE-FG03-94ER40833 and T.J.W. by DOE grant DE-FG05-85ER40226. N.F.B., S.P., and T.J.W. thank the Kavli Institute for Theoretical Physics at the University of California, Santa Barbara, for support and hospitality.

[1] E. Andres *et al.*, Nature (London) **410**, 441 (2001).
[2] I.A. Belolaptikov *et al.*, Astropart. Phys. **7**, 263 (1997); V.A. Balkanov *et al.*, *ibid.* **12**, 75 (1999); **14**, 61 (2000).
[3] J. Ahrens *et al.*, Phys. Rev. D **66**, 012005 (2002); J. Ahrens *et al.*, *ibid.* **67**, 012003 (2003); J. Ahrens *et al.*, Astrophys. J. **583**, 1040 (2003); J. Ahrens, Phys. Rev. Lett. **90**, 251101 (2003).
[4] S.W. Barwick, astro-ph/0211269.
[5] J. Ahrens *et al.*, astro-ph/0305196; IceCube Preliminary Design Document, available at http://icecube.wisc.edu/science/sci-tech-docs/; http://icecube.wisc.edu/
[6] T. Montaruli, physics/0306057.
[7] S.E. Tzamarias, Nucl. Instrum. Methods Phys. Res. A **502**, 150 (2003).
[8] A. Roberts, Rev. Mod. Phys. **64**, 259 (1992); P.C. Bosetti, Nucl. Phys. B (Proc. Suppl.) **48**, 466 (1996).
[9] F. Ameli, M. Bonori, and F. Massa, Eur. Phys. J. C **25**, 67 (2002).
[10] D.J. Bird *et al.*, Astrophys. J. **424**, 491 (1994).
[11] N. Hayashida *et al.*, Astrophys. J. **522**, 225 (1999).
[12] C. Tyler, A.V. Olinto, and G. Sigl, Phys. Rev. D **63**, 055001 (2001); L.A. Anchordoqui, J.L. Feng, H. Goldberg, and A.D. Shapere, *ibid.* **66**, 103002 (2002).
[13] T. Abu-Zayyad *et al.*, astro-ph/0208243; astro-ph/0208301.
[14] K.S. Capelle, J.W. Cronin, G. Parente, and E. Zas, Astropart. Phys. **8**, 321 (1998); J. Blumer, J. Phys. G **29**, 867 (2003).
[15] A. Petrolini, Nucl. Phys. B (Proc. Suppl.) **113**, 329 (2002); http://www.euso-mission.org; http://aquila.lbl.gov/EUSO/
[16] http://owl.gsfc.nasa.gov/
[17] G.A. Askaryan, Zh. Eksp. Teor. Fiz. **41**, 616 (1961) [Sov. Phys. JETP **14**, 441 (1962)].
[18] G.M. Frichter, J.P. Ralston, and D.W. McKay, Phys. Rev. D **53**, 1684 (1996); I. Kravchenko *et al.*, Astropart. Phys. **19**, 15 (2003); I. Kravchenko *et al.*, astro-ph/0206371; I. Kravchenko *et al.*, astro-ph/0306408.
[19] http://www.ps.uci.edu/~anita/
[20] G. Domokos and S. Kovesi-Domokos, hep-ph/9805221; D. Fargion, Astrophys. J. **570**, 909 (2002); X. Bertou, P. Billoir, O. Deligny, C. Lachaud, and A. Letessier-Selvon, Astropart. Phys. **17**, 183 (2002); J.L. Feng, P. Fisher, F. Wilczek, and T.M. Yu, Phys. Rev. Lett. **88**, 161102 (2002); A. Kusenko and T.J. Weiler, *ibid.* **88**, 161101 (2002).
[21] P.W. Gorham, K.M. Liewer, C.J. Naudet, D.P. Saltzberg, and D.R. Williams, astro-ph/0102435.
[22] P. Gorham, D. Saltzberg, A. Odian, D. Williams, D. Besson, G. Frichter, and S. Tantawi, Nucl. Instrum. Methods Phys. Res. A **490**, 476 (2002).
[23] T.K. Gaisser, F. Halzen, and T. Stanev, Phys. Rep. **258**, 173 (1995); **271**, 355(E) (1996); J.G. Learned and K. Mannheim, Annu. Rev. Nucl. Part. Sci. **50**, 679 (2000); F. Halzen and D. Hooper, Rep. Prog. Phys. **65**, 1025 (2002); I.F. Albuquerque, J. Lamoureux, and G.F. Smoot, Astrophys. J., Suppl. Ser. **141**, 195 (2002); C. Spiering, J. Phys. G **29**, 843 (2003).
[24] J.G. Learned and S. Pakvasa, Astropart. Phys. **3**, 267 (1995).
[25] H. Athar, M. Jezabek, and O. Yasuda, Phys. Rev. D **62**, 103007 (2000); D.V. Ahluwalia, Mod. Phys. Lett. A **16**, 917 (2001).
[26] J.P. Rachen and P. Meszaros, Phys. Rev. D **58**, 123005 (1998).
[27] J.F. Beacom, N.F. Bell, D. Hooper, S. Pakvasa, and T.J. Weiler, Phys. Rev. Lett. **90**, 181301 (2003); hep-ph/0309267.
[28] G. Barenboim and C. Quigg, Phys. Rev. D **67**, 073024 (2003).
[29] R.M. Crocker, F. Melia, and R.R. Volkas, Astrophys. J., Suppl. Ser. **130**, 339 (2000); **141**, 147 (2002); V. Berezinsky, M. Narayan, and F. Vissani, Nucl. Phys. **B658**, 254 (2003); J.F. Beacom, N.F. Bell, D. Hooper, J.G. Learned, S. Pakvasa, and T.J. Weiler, hep-ph/0307151.
[30] V. Agrawal, T.K. Gaisser, P. Lipari, and T. Stanev, Phys. Rev. D **53**, 1314 (1996).
[31] E. Waxman and J.N. Bahcall, Phys. Rev. Lett. **78**, 2292 (1997); F. Halzen, astro-ph/9810368; D. Guetta, D. Hooper, J. Alvarez-Muniz, F. Halzen, and E. Reuveni, astro-ph/0302524.
[32] N. Gupta, Phys. Lett. B **541**, 16 (2002); Phys. Rev. D **68**, 063006 (2003).
[33] T. Gaisser, *Cosmic Rays and Particle Physics* (Cambridge University Press, Cambridge, England, 1991); S. Iyer Dutta, M.H. Reno, I. Sarcevic, and D. Seckel, Phys. Rev. D **63**, 094020 (2001); D.E. Groom, N.V. Mokhov, and S.I. Striganov, At. Data Nucl. Data Tables **78**, 183 (2001).
[34] R.P. Kokoulin and A.A. Petrukhin, Nucl. Instrum. Methods Phys. Res. A **263**, 468 (1988); P. Lipari and T. Stanev, Phys. Rev. D **44**, 3543 (1991); A.P. Chikkatur *et al.*, Z. Phys. C **74**, 279 (1997).
[35] J.F. Beacom, P. Crotty, and E.W. Kolb, Phys. Rev. D **66**, 021302(R) (2002).

[36] R. Gandhi, C. Quigg, M.H. Reno, and I. Sarcevic, Phys. Rev. D **58**, 093009 (1998).
[37] E. Waxman and J.N. Bahcall, Phys. Rev. D **59**, 023002 (1999); J.N. Bahcall and E. Waxman, *ibid.* **64**, 023002 (2001).
[38] J.P. Rachen, R.J. Protheroe, and K. Mannheim, astro-ph/9908031; K. Mannheim, R.J. Protheroe, and J.P. Rachen, Phys. Rev. D **63**, 023003 (2001).
[39] V.S. Berezinsky and V.I. Dokuchaev, Astropart. Phys. **15**, 87 (2001).
[40] F. Halzen and D. Saltzberg, Phys. Rev. Lett. **81**, 4305 (1998).
[41] S.I. Dutta, M.H. Reno, and I. Sarcevic, Phys. Rev. D **66**, 077302 (2002); E. Bugaev, T. Montaruli, and I. Sokalski, astro-ph/0305284.
[42] H. Athar, G. Parente, and E. Zas, Phys. Rev. D **62**, 093010 (2000).
[43] J. Alvarez-Muniz and F. Halzen, ''Detection of Tau Neutrinos in IceCube,'' 1999, available at http://icecube.wisc.edu/science/sci-tech-docs/
[44] D. Hooper, H. Nunokawa, O.L. Peres, and R. Zukanovich Funchal, Phys. Rev. D **67**, 013001 (2003).
[45] S.I. Dutta, M.H. Reno, and I. Sarcevic, Phys. Rev. D **62**, 123001 (2000).